

SOUTHWESTERN UNIVERSITY

Brown Working Papers in the Arts & Sciences

Volume X

(2010)



Characterization of Hurricane Gust factors using Observed and Simulated Data

Rebecca Paulsen Edwards
Department of Physics, Southwestern University
Georgetown, TX 78627
edwardsr@southwestern.edu

John L. Schroeder
Department of Atmospheric Sciences, Texas Tech University

Recommended Citation:

Edwards, Rebecca Paulsen and John L. Schroeder, (2010) "Characterization of Hurricane Gust factors using Observed and Simulated Data," Brown Working Papers in the Arts and Sciences, Southwestern University, Vol. X. Available at: <http://www.southwestern.edu/academics/bwp/vol10/Edwards-2010.pdf>.

Characterization of Hurricane Gust factors using Observed and Simulated Data

Rebecca Paulsen Edwards, *Department of Physics, Southwestern University*
John L. Schroeder, *Department of Atmospheric Sciences, Texas Tech University*

1. Introduction

The nature of wind in the hurricane boundary layer continues to be the subject of study and debate. Questions of whether there are differences between tropical cyclone wind and wind generated synoptically in an extratropical environment have been addressed in numerous studies (Durst, 1960; Kraymer and Marshall, 1992; Miller, 2006; Paulsen and Schroeder, 2004; Sparks and Huang, 1999; Vickery and Skerlj, 2005). In particular, these studies have focused on the behavior of the gust factor (GF), which is the ratio of a peak wind speed of a certain duration and a mean wind speed of a certain duration (e.g. a 2-second/10-minute GF). The exploration of this question is complicated by a relative lack of data at extreme wind speeds. The recent deployment of mobile instrumentation platforms into several major hurricanes (e.g., Ivan, Katrina, and Rita) has resulted in additional data from higher wind speed events. This project seeks to combine the newly available data with historical, lower wind speed tropical cyclone data, extratropical wind data, and unique analysis techniques to make a contribution to furthering our understanding of hurricane boundary layer turbulence.

2. Historical Work

Questions regarding the structure of the near-surface hurricane boundary layer have been the subject of a number of studies conducted within the last five decades. Much has been learned from these studies, including that convection plays a role in boundary layer structure and exposure differences must be accounted for when making comparisons among different data sources. However a number of questions have also arisen from the results of the previous work.

In 1992 Kraymer and Marshall used data from four hurricanes (Frederic, Alicia, Elena, and Hugo) to determine whether relationships developed using extratropical data could also be used in winds generated by hurricanes. They found a mean GF from tropical cyclone wind of 1.55 and compared it with an earlier study by Durst (1960), who found a mean GF of 1.40 in an extratropical environment. They concluded that GFs were higher for tropical relative to extratropical winds.

Ashcroft (1994) noted a dependence of the gust ratio (a similar statistic to the gust factor) on the terrain roughness. For the longer duration gust ratios, Ashcroft found a slight but statistically significant decrease of the gust ratio with increasing wind speed. Sparks and Huang (1999, 2001) and Vickery and Skerlj (2005) also attributed the different results found by Kraymer and Marshall and Durst to differences in terrain exposure. Vickery and Skerlj further noted little difference between the tropical and extratropical gust factor at elevated wind speeds and a decrease in the GF with increasing wind speed. On the other hand, Sharma and Richards (1999) found tropical cyclones to be convectively unstable and determined that convective instability was the reason for the higher gust factors found for tropical cyclone wind relative to extratropical wind.

Paulsen and Schroeder (2004) emphasized the importance of stratifying data by roughness before making comparisons between tropical and extratropical wind data.

However, even after such stratification was performed they found slightly higher GFs for the tropical data set relative to the extratropical. In 2006 Miller confirmed the difference between the tropical and extratropical distributions and found that the difference diminished with increasing wind speed.

3. Methodology

3.1 Full-Scale Data Collection

The same set of five instrumented towers was used to collect both the tropical and extratropical wind speed and direction data. Two of the towers were designed specifically for use in the hurricane environment. These two towers, dubbed WEMITE #1 and WEMITE #2, were ruggedized to withstand sustained wind speeds of 67 m s^{-1} . WEMITE #1 and WEMITE #2 feature anemometers at three and five levels, respectively. Three non-ruggedized portable meteorological towers (PMT) with instrumentation at only one level (10 m) were added to the project in 2001. In addition to wind speed and direction, each of the five towers also sampled temperature, relative humidity, and barometric pressure data. Each tower was capable of sampling at frequencies of 2-10 Hz, but the actual sampling rate used varied by platform, storm, and experiment. An outline of the three types of towers and the instrumentation present on each is provided in Table 1.

Table 1. Summary of instrument towers used for collection of full-scale data.

Quantity	Tower Description	Instrumentation (as of 2003)
1	<ul style="list-style-type: none"> • "WEMITE 2" • Trailer mounted 15 m tower • Can withstand sustained wind speeds of up to 67 m s^{-1} • Sampling Rate: 10 Hz 	<ul style="list-style-type: none"> • 5 RM Young Wind Monitors (2.13 m, 3.96 m, 6.1 m, 10.06 m, and 15.24 m) • 1 Sonic Anemometer (10.06 m) • 1 Vertical Anemometer (3.96 m) • BP, T, and RH sensors
1	<ul style="list-style-type: none"> • "WEMITE 1" • Trailer mounted 10 m tower • Can withstand sustained wind speeds of up to 67 m s^{-1} • Sampling Rate: 10 Hz 	<ul style="list-style-type: none"> • 3 RM Young Wind Monitors (3.05 m, 6.1 m, and 10.06 m) • 1 Sonic Anemometer (10.06 m) • 1 Vertical Anemometer (10 m) • BP, T, and RH sensors
3	<ul style="list-style-type: none"> • 10m non-ruggedized portable tower • Sampling Rate: 2-10 Hz 	<ul style="list-style-type: none"> • 1 RM Young Wind Monitor (10 m) • 1 Vertical Anemometer (10 m) • BP, T, and RH sensors

The instrument used on all five towers to collect wind speed and direction data was an R.M. Young Wind Monitor Model 05106. It is a propeller-vane anemometer which measures both wind speed and direction. The propeller maintains a distance constant of 2.7 m for 63% recovery. The inherent inertia present in the anemometer due to its moving components compromises the ability to measure small-scale (high-frequency) energy of the wind. This limitation does not affect the primary statistics examined in this study, the 2-second/10-minute and 2-second/5-minute GF. In Schroeder and Smith (2003) a more complete discussion of the limitations of the R.M. Young Wind Monitor used in this study is provided.

Tropical Cyclone Data

The details of the fourteen hurricane deployments during which tropical data were collected are provided in Table 2. Although an effort was made to deploy towers in an open, airport exposure to minimize upwind obstructions in all directions, deployment in open exposure was not possible in every case; the dataset contains information from a variety of roughness exposures, including marine and rough exposures as classified by Wieringa (1993). Transitional flow regimes which occur downstream from a change in terrain are also inherent to the data.

Table 2. Storm names and associated deployment locations (1998-2005) W1: WEMITE #1, W2: WEMITE #2.

Storm/Year	Platform	Location	Storm/Year	Platform	Location
Bonnie/1998	W1	Wilmington, NC	Ivan/2004	W1	Gulf Shores, AL
Bret/1999	W1	Corpus Christi, TX		W2	Fairhope, AL
	W2	Kingsville, TX		PMT-B	Gulfport, MS
Charley/1998	W1	Rockport, TX		PMT-C	Destin, FL
Dennis/1999	W1	Atlantic, NC	Lili/2002	W2	Cote Blanche, LA
	W2	Beaufort, NC	Isabel/2003	W1	Beaufort, NC
Earl/1998	W1	Panama City, FL		W2	Atlantic, NC
Floyd/1999	W1	Southport, NC		PMT-W	New Bern, NC
	W2	Wilmington, NC	Katrina/2005	W1	Vacherie, LA
Frances/2004	W1	Vero Beach, FL		PMT-W	Stennis, MS
	W2	Melbourne, FL		PMT-C	Slidell, LA
	PMT-B	Titusville, FL		Rita/2005	W2
PMT-C	Ft. Pierce, FL	PMT-B	Orange, TX		
Gabrielle/2001	W2	Flagler Beach, FL	PMT-W		Anahuac, TX
Isidore/2002	W2	Gulfport, MS	PMT-C		Winnie, TX

Extratropical Data

The full-scale extratropical data used were collected during an experiment in 2002, when an array of seven towers was deployed in a north-south array along a runway at Reese Technology Center (a decommissioned Air Force base) west of Lubbock, Texas to document the kinematic and thermodynamic structure of hurricane outflows (Gast and Schroeder, 2003). Data were collected at a sampling rate of 2 Hz throughout May and June. The exposure at Reese Technology Center is primarily open, but some of the data reflects the presence of other exposures, with z_0 s both above and below those included in the open roughness regime.

Before data were included in the extratropical dataset, each record was examined for thunderstorm outflows. Thunderstorm winds are highly non-stationary and not appropriate for comparison with tropical cyclone data. Data collected on days when a thunderstorm occurred according to written records were removed. In addition, each record was visually examined for evidence that thunderstorm data might be present. If a sudden strong peak in the wind speed lasting less than 10 minutes and accompanied by an abrupt change in wind direction was observed, that record was classified as thunderstorm data and removed from the dataset. Once the thunderstorm data were removed from the extratropical dataset, each record was examined once again to check for instrument induced data spikes. Any sudden peak in any parameter of such a magnitude and of such short duration that it precludes physical explanation was classified as a spike. Any spikes that were identified were removed from the dataset by dividing the record into two records, one before and one after the spike.

3.2 Turbulence Parameters

A LabVIEW program was used to divide each wind speed time history into 10-minute segments then calculate various statistics including various means and peak wind speeds, meteorological parameters, and the GF, turbulence intensity (TI), and roughness length (z_0), which are discussed in more detail here.

Gust Factor

The GF is a ratio of the peak wind speed (\hat{u}) of a specified duration and the mean wind speed (\bar{u}) as in Equation 1. The mean wind speed was determined by taking the average value of the wind speed data segment. The peak gust was determined by using a sliding window filtering technique (width defined by the gust duration) for each segment of data. The largest filtered value was selected as the peak gust.

$$GF = \frac{\hat{u}}{\bar{u}} \quad (1)$$

Turbulence Intensity

The TI is calculated by dividing the standard deviation (σ) of a segment of data by the mean wind speed (\bar{u}) of the same segment as in Equation 2.

$$TI = \frac{\sigma}{\bar{u}} \quad (2)$$

Roughness Length

The z_0 is used to describe the roughness of the exposure upstream from the observation site. It can be calculated using several different methods, but the method which was chosen for this study was the turbulence intensity (TI) method. The TI method consists of calculating z_0 directly from the turbulence intensity (TI) and the anemometer height (z) using Equation 3.

$$Z_o = \exp\left[\ln(z) - \frac{1}{TI}\right] \quad (3)$$

The TI method assumes a log-law profile and that the ratio of the standard deviation of the wind record to the friction velocity is 2.5 (Beljaars, 1987).

When multiple anemometer heights are available, z_0 can be calculated assuming the log-law profile. This method is completed by plotting the natural log of the anemometer heights versus the observed mean wind speeds acquired at each of those heights as shown in Figure 5.1.3.1. z_0 is then obtained from the y-intercept of the least squares fit for those points.

3.3 Stratification by Roughness

Because turbulence parameters are heavily dependent on terrain roughness, stratifying by roughness has proved to be critical when comparing turbulence parameters for different storms and different locations (Paulsen and Schroeder, 2004). All of the data were stratified into the four roughness regimes seen in Table 3 based on each segment's z_0 value.

Table 3. Roughness regimes and associated roughness length values (reproduced from Paulsen and Schroeder, 2005).

Name	Roughness Length (m)
Smooth	0.005-0.0199
Open	0.02-0.0499
Open to Roughly Open	0.05-0.0899
Roughly Open to Rough	0.09-0.1899

3.4 Generation of Simulated Data

Simulated wind speed time histories were created at specified wind speeds and standard deviations using an un-normalized form of the Universal Spectrum for wind (Geurts, 1997). Simulated data provides a control case, free from the influences of convection, instrument limitations, and transitional flow and is useful for identifying differences which may exist between tropical and extratropical flow. Additionally, simulated data can be created at wind speeds greater than those available observationally.

The Universal Spectrum

The universal spectra (Geurts, 1997) are non-dimensional theoretical spectra for wind based on a neutral atmospheric boundary layer. The expression for the universal spectra is given in Equation 4.

$$\frac{nS_{II}}{\sigma_i^2} = \frac{Af^\gamma}{(C + Bf^\alpha)^\beta}, \quad (4)$$

where:

$f = n \times z / u_m$ = normalized frequency

n = frequency

z = observation height

u_m = mean wind speed

σ^2 = variance of wind speed

S_{II} = spectral density function

and the coefficients α , β , and γ , and A, B, and C are provided in Table 4.

Table 4. Universal spectra coefficients (Tieleman 1995).

	FSU terrain: C=1 $\alpha = 5/3, \beta = 1, \gamma = 1$		Perturbed terrain: C=1 $\alpha = 1, \beta = 5/3, \gamma = 1$		Kaimal: C=1 $\alpha = 1, \beta = 5/3, \gamma = 1$	
	A	B	A	B	A	B
S_{uu}	20.53	475.1	40.42	60.62	21.66	33
S_{vv}	6.83	75.84	13.44	20.16	5.37	9.5
S_{ww}	1.67	7.23	3.28	4.92	1.14	5.3

Three sets of coefficients (Table 4.1), each suited for a different type of terrain, were available for the Universal Spectra. One terrain type of terrain, described as “perturbed terrain” is described in Geurts (1997) as “FSU [flat, smooth, uniform] terrain with incidental higher obstacles.” There are several reasons the perturbed terrain model was chosen for this study. It was found in Tieleman (1995) that only a few isolated obstacles within several kilometers upwind of the observation site are enough that the terrain could not be classified as FSU. Given the inherent time limitations when deploying the instrumentation in the tropical environment, it was not possible to locate deployment sites that met the strict FSU criteria. Comparisons made by Loruso et al. (2008) between observed tropical data and the universal spectrum indicate that the perturbed wind spectrum fits the observed spectrum better than either the FSU or Kaimal models. Comparisons of the tropical and extratropical observed spectra with spectra based on data created using the perturbed terrain spectrum also show reasonable agreement.

Un-normalization of Universal Spectrum

One limitation of the set of tropical and extratropical observed data is a relative scarcity of data recorded with mean wind speeds above 30 m s^{-1} . A primary objective of this project was to create wind speed time histories at a variety of wind speeds, both high and low. A benefit of using the universal spectra to create artificial time histories is that they can be scaled (un-normalized) to represent wind data collected at a specific mean wind speed and standard deviations. The process for un-normalizing the universal spectrum is as follows:

1. The quantity f , which is the frequency, n , normalized by z/u_m , was multiplied by u_m/z each time it appears in the universal spectrum equation. u_m represented the specified mean wind speed and z , the observation height, was set to 10 m in all cases to match the observation height of the observed tropical and extratropical data.
2. Multiply both sides of the resulting equation by $\sigma^2 / (n/2)$ where σ^2 is the variance (Mean wind speeds and corresponding standard deviations are listed in Table XXX). n is divided by two to account for the fact that a two-sided spectrum will be created instead of the one-sided spectrum specified by the original equation.

The resulting equation, which was used to generate time histories of artificial data at a specified wind speed and standard deviation, is given as Equation 5.

$$S_{ii} = \left[\frac{A \cdot \left(\frac{u_m \cdot n}{z} \right)^\gamma}{\left(C + B \left[\frac{u_m \cdot n}{z} \right]^\alpha \right)^\beta} \right] \times \frac{\sigma^2}{(n/2)} \quad (5)$$

Selection of Fundamental Frequency and Frequency Resolution

The range of frequencies over which each un-normalized spectrum was created and the frequency resolution, df , were chosen to best capture the entire range of frequencies described by the spectrum. The fundamental frequency, ff , was established by first finding the normalized frequency on the low-frequency end at which the value of S was very low (10⁻⁴). Next the range of frequencies from 0 to the Nyquist, fN , was divided into equal increments of df , $f1, f2, \dots, fN$, such that $f1$ was equal to ff . To simulate a sampling rate of 10 Hz, fN was set to 5 Hz. 10 Hz was the sampling rate at which much of the observed tropical data were collected. Using these constraints, the spectrum was created at 106 individual frequencies ranging from 0-5 Hz.

Generation of Artificial Time Series

The standard deviation corresponding to each mean wind speed was found using the turbulence intensity associated with an observation height of 10 m and a z_o of 0.035 m, the center of the open roughness regime range. The turbulence intensity was found using Equation 6. Mean wind speeds at which simulated time histories were created and corresponding standard deviations are found in Table 5.

$$Z_o = \exp \left[\ln(z) - \frac{1}{TI} \right] \quad (6)$$

Table 5. Mean wind speeds (\bar{u}) and corresponding standard deviations (σ) used to generate artificial data.

\bar{u} (m s ⁻¹)	σ (m s ⁻¹)
10	1.77
15	2.65
20	3.54
25	4.42
30	5.30
35	6.19
40	7.07
45	7.96
50	8.84

The un-normalized spectrum provided only the magnitudes needed to generate the artificial time series. To create many different unique time series based on the same spectrum, a set of randomized phase values were generated using a normally distributed random number generator in Matlab, then combined with the magnitudes provided by the spectrum. A unique time history could then be created from the spectrum using an inverse Fast Fourier transform (IFFT). Each time history created was 10⁶ values in

length, a number bound by the required frequency resolution, Nyquist frequency, and fundamental frequency. To create a longer time history at each mean wind speed, six time histories were created and strung together to result in one-hundred ten-minute segments of data in each time history.

Modification of the Universal Spectrum

Two modifications were made to the original universal spectrum to make its spectrum a better match to the observed data. First, energy was removed from the high-frequency end of the spectrum to simulate the signal attenuation that is caused by the limitations of the mechanical anemometer used to collect the full-scale data. The transfer function used to modify the spectrum is found in Equation 7 (DeFelice 1998).

$$A = \frac{1}{\sqrt{1 + (\tau \cdot \omega)^2}} \quad (7)$$

where:

$$\delta u = I_u * \bar{u}$$

$$L = 2.7 \text{ m (a property of the anemometer)}$$

$$\tau = \frac{L}{\delta u}$$

and ω is the angular frequency in radians per second.

Second, energy was added to the low-frequency end of the spectrum to simulate a low-frequency feature that has been observed in the tropical wind field (Lorsolo et al., 2005). Based on Lorsolo et al. the frequency at which the additional energy was applied was based on the mean wind speed (u) and chosen to be $fL=0.0006*u$. Once fL was determined, a trapezoidal bump 500 samples in width was applied to modify the spectrum. Both transfer functions were applied before the randomized phase was incorporated. The modified simulated data were then created in the same manner as the original simulated data. In comparisons of the original simulated data and PSDs with the modified-simulated data and PSDs (Figure 1), improved agreement is readily apparent, particularly on the high-frequency end of the spectrum.

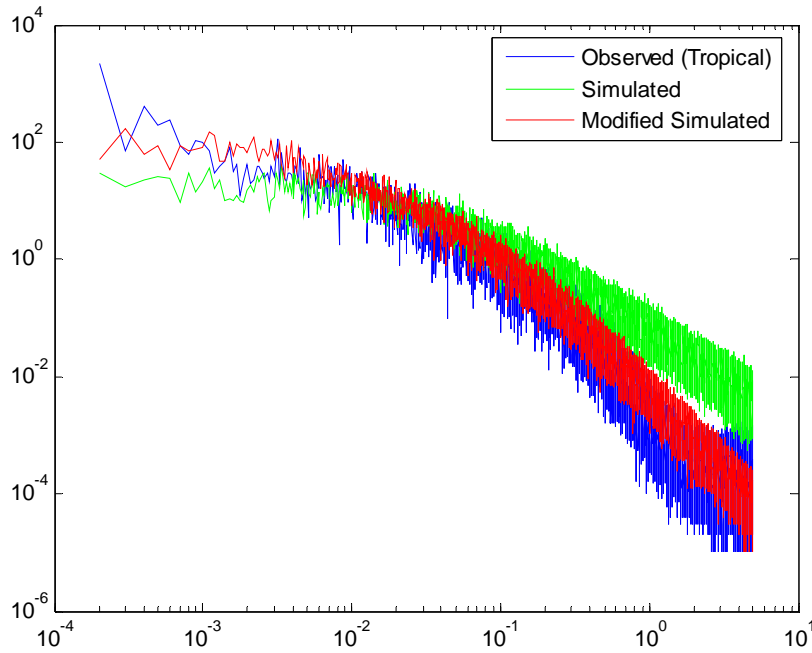


Figure 1. Normalized PSDs for samples of observed, simulated, and modified-simulated data.

3.5 Verification of Simulated Data

The validity of the artificial data was evaluated in three ways. First, an averaged, normalized power spectral density (PSD) based on a sample of artificial data was compared with the original universal spectrum (Figure 2). The shapes of the two normalized spectrums show good agreement with the exception of the extra noise present in the artificial data spectrum due to the randomized phase added to the base spectrum. This result verifies that the underlying universal spectrum is maintained during the un-normalization process. Next, a PSD was created for a 20-minute sample of each artificial data set. Those PSDs were then compared with those of a sample of observed data (Figure 4.3.3.2). Each time history's PSD bore a reasonable resemblance to the PSD of observed data with the expected exception of the shape of the spectrum on the high-frequency end. This difference was caused by the instrument limitation referenced earlier. Improved agreement between observed and simulated PSDs (Figure 1) is seen following modification of the universal spectrum to reflect this limitation. Finally, the area under the PSD (which was normalized by the variance of the time series) was found to ensure that it was equal to one in accordance with the definition of a one-sided spectrum, shown in Equation 8 (Geurts, 1997).

$$\sigma_i^2 = \int_0^{\infty} S_{ii}(n)dn \quad (8)$$

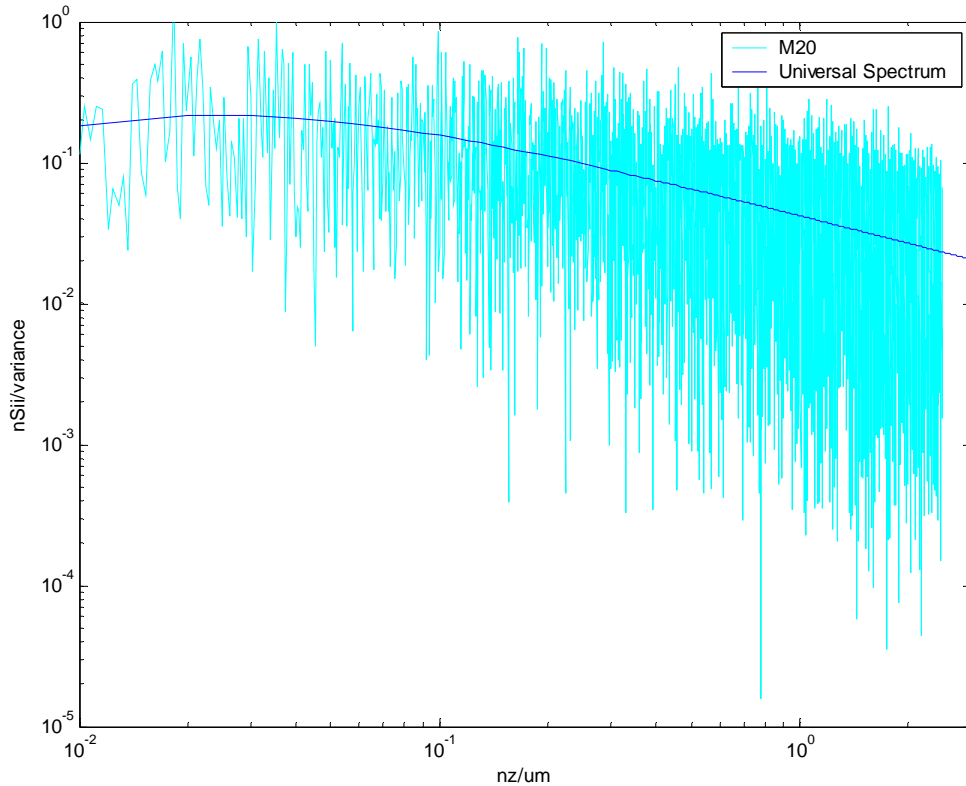


Figure 2. Comparison of the normalized universal spectrum for perturbed terrain (Geurts, 1997) with the normalized spectrum created from a sample of data from the M20 data set.

Comparison of Input and Resultant Wind Speed Values

Of the 900 10-minute segments of data created, 781 had z_{0s} that classified them as belonging to the open regime and 29 were classified as belonging to the open to roughly open regime. The remaining 90 segments were classified as belonging to the smooth regime. The large number of segments in the open roughness regime data set supports the earlier conclusion that the description of perturbed terrain identified most closely with the open exposure found at many of the deployment sites where observational data were collected.

Table 6 lists the input mean and standard deviation used to create each data set and the mean and standard deviation taken from the resultant time history. Data sets are identified by an “M” and followed by the value of the mean wind speed specified when the data set was created. For example, the “M10” data set was created using a 10-min mean wind speed of 10 m s^{-1} . As can be seen in the table, the means and standard deviations for the artificial data time histories showed good agreement with the mean and standard deviation values specified when the data were created. The resultant mean wind speed values are within a tenth of a meter per second of the input value for each case. The resultant standard deviation values are consistently lower than the input standard deviation values. Although the magnitude of the difference increases with wind speed from a difference of 0.02 m s^{-1} for the M10 data set to a difference of 0.3 m s^{-1} for the M50 data set, the difference is modest in terms of percent difference. The results were

similar in the case of the modified-simulated data, with percent differences between mean and input standard deviations ranging from 0.04 and 5.43%.

Table 6. Comparison of input and resultant mean wind speed (ws) and standard deviation (stdev) values for each artificial dataset created.

Input		Simulated			Modified-Simulated		
Mean	Stdev	Mean	Stdev	%diff (stdev)	Mean	Stdev	%diff (stdev)
10	1.77	10.04	1.75	1.14	10.02	1.68	5.43
15	2.65	15.01	2.62	1.14	14.94	2.63	0.71
20	3.54	20.08	3.48	1.71	19.87	3.46	2.33
25	4.42	24.94	4.36	1.37	25.07	4.46	0.91
30	5.3	29.91	5.15	2.87	29.97	5.32	0.39
35	6.19	34.90	6.00	3.12	34.65	6.16	0.47
40	7.07	40.07	6.83	3.45	40.20	7.24	2.41
45	7.96	44.98	7.71	3.19	45.27	7.96	0.04
50	8.84	50.05	8.54	3.45	50.22	8.99	1.69

4. Results and Discussion

Data from fourteen landfalling tropical cyclones and synoptically generated extratropical systems were compared with

4.1 Comparison of Observed and Simulated Time Histories

Samples of observed (tropical and extratropical) and simulated time histories are provided in Figure 3. The apparent difference in high-frequency energy between the tropical and extratropical time histories is caused in part by the lower sampling rate at which the extratropical data were collected (2 Hz for the extratropical data vs. 10 Hz for the tropical). The extratropical data's lower Nyquist frequency means that variation above 1 Hz will not be resolved when data are collected. On the other hand, the increased amount of high-frequency energy visible in the simulated time history (3rd panel, Figure 3), is due to the additional high-frequency energy present in the universal spectrum that is not present in the observed data due to instrument limitations. The modified-simulated data (Panel 4) reflects both the reduction in high-frequency energy and the low-frequency undulation induced by the two transfer functions and qualitatively is a good match with the two types of observed data.

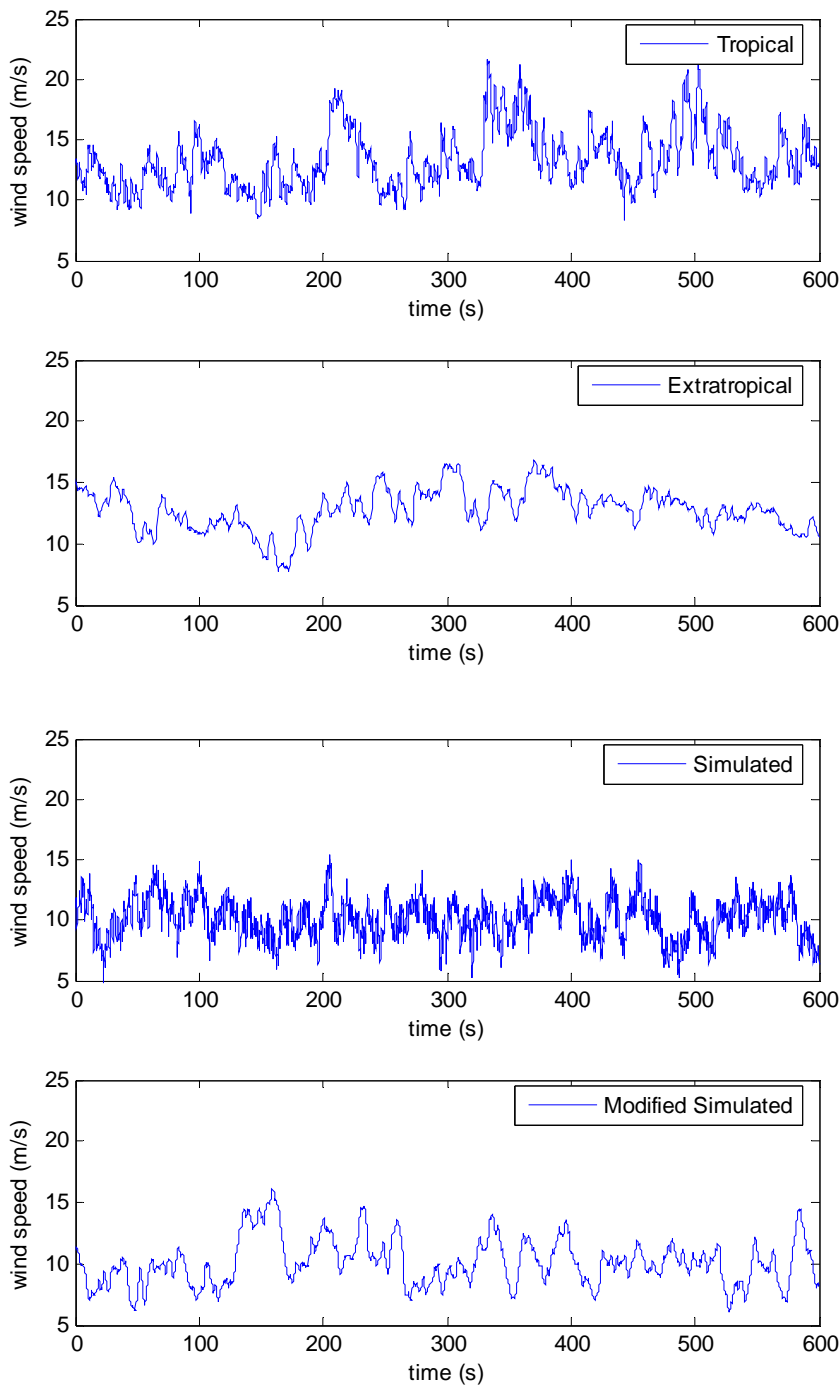


Figure 3. Comparison of time histories from observed tropical data (top), observed extratropical data (center), and from simulated data (bottom).

4.2 Gust Factor Results from Observed and Simulated Data

2-second/10-minute GFs were generated for four types of data—tropical, extratropical, simulated, and modified-simulated and compared. Because the wind field is more susceptible to thermally driven convection at low wind speeds and because the scope of this study is mechanical shearing of wind at higher wind speeds, data with a

mean wind speed of less than 5 m s^{-1} from both the tropical and extratropical environments were discarded for this study. Simulated data were not created at 5 m s^{-1} .

The mean 2-sec/10-minute GF for the tropical dataset, open roughness regime, was 1.49. The mean 2-sec/10-minute GF found for the extratropical, open roughness regime dataset, 1.44. Both values fall between the GF values found by Durst (1960), 1.40, and Krayner and Marshall (1992), 1.55. The corresponding values for the simulated and modified-simulated data were 1.44 and 1.45, respectively. All mean GF values for each tropical, extratropical, simulated, and modified-simulated data set in each of the roughness regimes are provided in Table 7. Because it was created based on a z_0 representative of the open roughness regime, the majority (781 of 900 10-minute segments) of the simulated data falls into the open roughness regime. Within each roughness regime, the mean GF is found to be higher for the tropical, relative to the extratropical data. Mean GFs from the simulated data also fall below those of the tropical values.

Table 7. Summary of mean GF values from the tropical (T), extratropical (ET), simulated (S), and modified-simulated (M-S) datasets.

	2-sec/10-min mean GF				Sample Size			
	T	ET	S	M-S	T	ET	S	M-S
Smooth	1.41	1.37	1.39	1.41	989	234	90	113
Open	1.49	1.44	1.44	1.45	1702	555	781	377
Open to Roughly Open	1.57	1.51	1.50	1.52	1045	225	29	49
Roughly Open to Rough	1.67	1.56	---	---	976	185	0	0

Presented in Figure 4 are histograms of the GF distributions for the tropical, extratropical, simulated, and modified-simulated data within the open roughness regime. The histograms indicate additional similarities between the simulated and extratropical GF distributions. Specifically, the modified-simulated data and tropical data share a similar broad shape with a further-right center. On the other hand, the extratropical GF distribution and basic simulated data show good agreement with one another. The further right position of the modified-simulated and tropical histograms relative to the basic simulated and extratropical histograms is reflected in the tabular GF results found in Table 6. These similarities suggest that redistributing energy from the high- to the low-frequency end of the spectrum slightly increases the resulting GFs. Further, the additional low-frequency energy may be part of the reason for the difference in GF seen between the tropical and extratropical observed data.

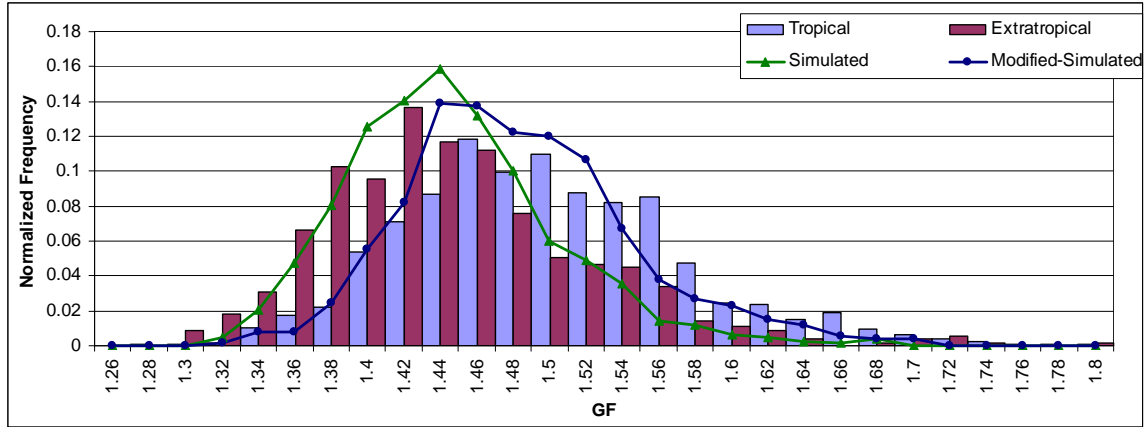


Figure 4. Histogram of GF distributions for the tropical, extratropical, simulated, and modified-simulated data from the open roughness regime.

5. Discussion

Wind speed time series created using the universal spectrum bear a reasonable resemblance to observed wind data, both qualitatively and in the resulting GF statistics and PSDs. There are a number of uses for simulated data. First, it can be created at wind speeds higher than those easily obtained observationally which enables better understanding of the behavior of the wind field at high wind speeds. Second, simulated wind data is representative of an idealized environment, free from the influence of convection, obstacles upstream from the observing instrument, and transitional flow. In this way, simulated data serves as a “control” data set, which is useful for uncovering differences among other data sets from different environments (i.e. the tropical and extratropical environments).

Comparisons made between the artificial and observed GF distributions reveal commonalities between the extratropical and simulated GF distributions while the distribution of the modified-simulated data resembled that of the tropical distribution. Additionally, the higher mean GF for the modified-simulated data set (open roughness regime) compared with the original simulated data set echoes the higher mean GF found in each tropical data set relative to the extratropical. This result suggests that the underlying difference between the tropical and extratropical data may lie in the additional low-frequency energy present in tropical cyclone wind documented in the full-scale data both in this study and others (Powell et al., 1996). However, the small magnitude of the resulting increase in mean GF suggest that additional factors are contributing to the increased GF in the tropical data as well.

6. Conclusions

Data collected from landfalling tropical cyclones and synoptically generated extratropical wind were compared with idealized simulated data created based on the universal spectrum. An additional dataset was also created using a spectrum for which energy was redistributed from the high- to the low-frequency end of the spectrum. Turbulence statistics were calculated for each data set and comparisons were made. The following conclusions can be drawn from this work:

- Simulating idealized wind speed time series using the universal spectrum with added randomized phase is an appropriate means of simulating wind speed time series from an idealized environment.
- Redistributing energy from the high- to the low-frequency end of the spectrum causes an increase in the resulting GF on the order of 0.01.
- Similarities between the extratropical and base simulated GF distributions and the tropical and modified-simulated GF distributions suggest that the higher GFs observed in the tropical relative to the extratropical data may be due in part to the additional low-frequency energy observed in the tropical wind spectrum observed by Lorsolo et al. However, the modest increase in GF from the base to the modified simulated data suggest that there are more factors at work.

References

- DeFelice, Thomas P. An introduction to meteorological instrumentation and measurement. Upper Saddle River, New Jersey: Prentice Hall, 1998.
- Durst, C.S., 1960: Wind speeds over short periods of time. *Meteor. Mag.*, 89, 181-187.
- Gast, K. D., and J. L. Schroeder, 2003: Supercell rear-flank downdraft as sampled in the 2003 thunderstorm outflow experiment. Preprints, 11th Int. Conf. on Wind Engineering, Lubbock, TX, Int. Assoc. for Wind Eng. and Amer. Assoc. for Wind Eng., 2233-2240.
- Guerts, C., 1997: Wind-induced pressure fluctuations on buildings. Technische Universiteit Eindhoven, Faculteit Bouwkunde, Vakgroep Constructief Ontwerpen, pp 30-34.
- Krayer, W. R., and R. D. Marshall, 1992: Gust factors applied to hurricane winds. *Bull. Amer. Meteor. Soc.*, 73, 613-617.
- Lorsolo, S., and J. L. Schroeder, 2006: "Tower and Doppler Radar Observations from the Boundary Layer of Hurricanes Isabel (2003) and Frances (2004)," Preprint, 27th Conference on Hurricanes and Tropical Meteorology, Monterrey California.
- Miller, C., 2006: Gust factors in hurricane and non-hurricane conditions. Preprints, 27th Conf. on Hurricanes and Tropical Meteorology, Monterey, CA, Amer. Meteor. Soc.
- Paulsen, R. M., J. L. Schroeder, M. R. Conder, and J. R. Howard, 2003; Further examination of hurricane gust factors, Proceedings, Eleventh International Conference on Wind Engineering, Lubbock, Texas, 2005-2012.
- Paulsen, B. M., and J. L. Schroeder, 2004: An examination of tropical and extratropical Gust factors and the associated wind speed histograms. *Journal of Applied Meteorology.*, 44, 270-280.
- Paulsen, B. M., and J. L. Schroeder, 2005: An examination of tropical and extratropical gust factors and the underlying wind speed histograms, *Journal of Applied Meteorology*, 44, 270-280.
- Schroeder, J. L., and D. A. Smith, 2003: Hurricane Bonnie wind flow characteristics. *Journal of Wind Engineering and Industrial Aerodynamics*, **91**, 767-789.
- Sharma, P. R., and P. J. Richards, 1999: A re-examination of the characteristics of tropical cyclone winds. *J. Wind Engineering and Industrial Aerodynamics*, 83, 21-23.
- Sparks, P.R., and Z. Huang, 1999: Wind speed characteristics in tropical cyclones. *Wind Engineering into the 21st Century – Proceedings of the Tenth International Conference on Wind Engineering*, A. Larson, G. L. Larose, and F. M. Livesey, Eds., A. A. Balkema, 343-350.

Sparks, P. R., and Z. Huang, 2001: Gust factors and surface-to-gradient wind-speed ratios in tropical cyclones. *Journal of Wind Engineering and Industrial Aerodynamics.*, 89, 1047-1058.

Tieleman, H. W., 1995: Universality of velocity spectra. *Journal of Wind Engineering and Industrial Aerodynamics*, 56, 55-69.

Vickery, P. J., and P. F. Skerlj, 2005: Hurricane gust factors revisited. *Journal of Structural Engineering*, 131, 825-832.